

Experimental Observation of Motion of Ions in a Resonantly Driven Plasma Wakefield Accelerator

M. Turner,¹ E. Walter,^{2,3} C. Amoedo,¹ N. Torrado,^{1,4} N. Lopes,⁴ A. Sublet,¹
M. Bergamaschi,⁵ J. Pucek,⁵ J. Mezger,⁵ N. van Gils,¹ L. Verra,^{1,*} G. Zevi Della
Porta,^{1,5} J. Farmer,⁵ A. Clairembaud,^{1,5} F. Pannell,⁶ E. Gschwendtner,¹ and P. Muggli⁵
(AWAKE Collaboration)

R. Agnello,⁷ C.C. Ahdida,¹ Y. Andrebe,⁷ O. Apsimon,^{8,9} R. Apsimon,^{9,10} J.M. Arnesano,¹ V. Bencini,^{1,11}
P. Blanchard,⁷ P.K. Blum,¹ P.N. Burrows,¹¹ B. Buttenschön,¹² A. Caldwell,⁵ M. Chung,¹³ D.A. Cooke,⁶ C. Davut,^{8,9}
G. Demeter,¹⁴ A.C. Dexter,^{9,10} S. Doebert,¹ A. Fasoli,⁷ R. Fonseca,^{15,4} I. Furno,⁷ E. Granados,¹ M. Granetzný,¹⁶
T. Graubner,¹⁷ O. Grulke,^{12,18} E. Guran,¹ J. Henderson,^{9,19} F. Jenko,² M.A. Kedves,¹⁴ F. Kraus,¹⁷ M. Krupa,¹
T. Lefevre,¹ L. Liang,^{8,9} S. Liu,²⁰ K. Lotov,^{21,22} M. Martinez Calderon,¹ S. Mazzoni,¹ P.I. Morales Guzmán,⁵
M. Moreira,⁴ T. Nechaeva,⁵ N. Okhotnikov,^{21,22} C. Pakuza,¹¹ A. Pardons,¹ K. Pepitone,²³ E. Poimendidou,¹
A. Pukhov,²⁴ R.L. Ramjiawan,^{1,11} L. Ranc,⁵ S. Rey,¹ R. Rossel,¹ H. Saberi,^{8,9} O. Schmitz,¹⁶ E. Senes,¹ F. Silva,²⁵
L. Silva,⁴ B. Spear,¹¹ C. Stollberg,⁷ C. Swain,^{9,26} A. Topaloudis,¹ P. Tuev,^{21,22} F. Velotti,¹ V. Verzilov,²⁰ J. Vieira,⁴
C. Welsch,^{9,26} M. Wendt,¹ M. Wing,⁶ J. Wolfenden,^{9,26} B. Woolley,¹ G. Xia,^{9,8} V. Yarygova,^{21,22} and M. Zepp¹⁶

¹CERN, 1211 Geneva 23, Switzerland

²Max Planck Institute for Plasma Physics, 85748 Garching, Germany

³Exzellenzcluster ORIGINS, 85748 Garching, Germany

⁴GoLP/Instituto de Plasmas e Fusão Nuclear, Instituto Superior Técnico,
Universidade de Lisboa, 1049-001 Lisbon, Portugal

⁵Max Planck Institute for Physics, 80805 Munich, Germany

⁶UCL, London WC1 6BT, United Kingdom

⁷Ecole Polytechnique Federale de Lausanne (EPFL),

Swiss Plasma Center (SPC), 1015 Lausanne, Switzerland

⁸University of Manchester M13 9PL, Manchester M13 9PL, United Kingdom

⁹Cockcroft Institute, Warrington WA4 4AD, United Kingdom

¹⁰Lancaster University, Lancaster LA1 4YB, United Kingdom

¹¹John Adams Institute, Oxford University, Oxford OX1 3RH, United Kingdom

¹²Max Planck Institute for Plasma Physics, 17491 Greifswald, Germany

¹³POSTECH, Pohang 37673, Republic of Korea

¹⁴HUN-REN Wigner Research Centre for Physics, Budapest, Hungary

¹⁵ISCTE - Instituto Universitário de Lisboa, 1049-001 Lisbon, Portugal

¹⁶University of Wisconsin, Madison, WI 53706, USA

¹⁷Philipps-Universität Marburg, 35032 Marburg, Germany

¹⁸Technical University of Denmark, 2800 Kgs. Lyngby, Denmark

¹⁹STFC/ASTeC, Daresbury Laboratory, Warrington WA4 4AD, United Kingdom

²⁰TRIUMF, Vancouver, BC V6T 2A3, Canada

²¹Budker Institute of Nuclear Physics SB RAS, 630090 Novosibirsk, Russia

²²Novosibirsk State University, 630090 Novosibirsk, Russia

²³Angstrom Laboratory, Department of Physics and Astronomy, 752 37 Uppsala, Sweden

²⁴Heinrich-Heine-Universität Düsseldorf, 40225 Düsseldorf, Germany

²⁵INESC-ID, Instituto Superior Técnico, Universidade de Lisboa, 1049-001 Lisbon, Portugal

²⁶University of Liverpool, Liverpool L69 7ZE, United Kingdom

(Dated: June 25, 2024)

We observe for the first time an effect on the driver caused by the motion of ions in a plasma wakefield accelerator. The effect manifests itself as a beam tail, which only occurs when sufficient motion of ions suppresses wakefields. By changing the plasma ions (helium, argon, xenon) in the experiment, we show that the effect depends inversely on the ion mass, as predicted from theory and simulations. Wakefields are driven resonantly by multiple bunches, and simulation results indicate that the ponderomotive force causes the motion of ions. In this case, the effect is also expected to depend on the amplitude of the wakefields, as also observed by varying the bunch charge.

* Present Address: INFN Laboratori Nazionali di Frascati, 00044 Frascati, Italy

Plasma wakefield acceleration is a novel and innovative concept for accelerating charged particles [1, 2]. Acceleration with gradients of tens of GeV/m [3, 4] has been experimentally demonstrated. As these gradients are significantly larger than those sustained by radio-frequency cavities (~ 100 MV/m), the concept has the potential to reduce the footprint of future high-energy linear accelerators.

In plasma wakefield accelerators, the accelerating structure is formed and sustained by plasma electrons, which oscillate collectively (with a plasma period τ_{pe} [5]) in a background of positively-charged plasma ions (often assumed to be immobile and uniformly distributed). Most commonly, wakefields are excited by a single, short and dense or intense driver (relativistic charged particle bunch or laser pulse) fitting within τ_{pe} . However, wakefields can also be excited resonantly by a train of less dense or intense drivers spaced at τ_{pe} . Such a driver train can be preformed [6, 7] or be the result of a self-modulation process [8–10]. In both schemes, a properly placed charged particle bunch (witness) is accelerated and focused by the wakefields.

With a single driver and the accelerated bunch in the same period of the wakefields, the accelerator usually operates in the blow-out regime [11]. In this case, a negatively-charged witness bunch travels in the uniform ion column left behind the driver, which provides an ideal restoring force profile, i.e., increasing linearly with distance from the axis. However, the force profile is modified when motion of ions, e.g. caused by the response to the impulse force from the fields of the driver or of the accelerated bunch, leads to a non-uniform ion density distribution within one period of the wakefields. This results in witness bunch emittance growth, whose magnitude may be unacceptable, especially in the context of a collider [12]. However, motion of ions has been proposed to be used in a positive way, i.e., to suppress the beam-hose instability [13, 14] that compromises the acceleration process [15, 16]. In that case, motion of ions is used to introduce a suppression mechanism similar to that in Balakin-Novokhatski-Smirnov (BNS) damping [15].

When using a train of drivers to excite wakefields resonantly, the witness bunch is placed not in the first, but in the n^{th} ($n > 1$) period of the wakefields, since the amplitude of the wakefields grows along the train. Therefore, the effect of the motion of ions over n periods must be considered. A new cause for the motion of ions may become dominant, i.e., the cumulative effect of the ponderomotive force of the wakefields themselves acting on the ions [17–19]. In this case, the motion of ions indirectly perturbs the acceleration process by perturbing the driving of the wakefields.

The expression for the ponderomotive force of a plasma wave of angular frequency $\omega = \omega_{pe}$ is [18]:

$$\mathbf{F}_p \cong -\frac{e^2}{4m_e\omega_{pe}^2}\nabla\tilde{W}_r^2, \quad (1)$$

where e is the electron charge, m_e is the electron mass, $\omega_{pe} = \sqrt{\frac{n_{pe}e^2}{\epsilon_0 m_e}}$ is the plasma electron angular frequency, n_{pe} is the plasma electron density, ϵ_0 is the vacuum dielectric constant and \tilde{W}_r is the envelope of the transverse wakefield. Using theory and simulations, the effects of \mathbf{F}_p and its dependencies can be quantified, as was done in Refs. [19] and [20]. In Ref. [19], the time along the bunch for the ion density perturbation to reach the initial density scales as $m_i^{1/2}$, where m_i is the ion mass. In Ref. [20], it was found that the time along the bunch for wavebreaking to occur as a result of motion of ions scales as $m_i^{1/3}$. In both cases the effect scales with the inverse of m_i and occurs earlier along the bunch with lighter ions. Additionally, Eq. 1 shows that $|\mathbf{F}_p|$ scales with the square of the envelope of the transverse wakefields \tilde{W}_r (for a fixed transverse bunch size σ_r , as W_r is zero on-axis and increases radially to a maximum value over a distance of approximately σ_r). The effect of the ponderomotive force on the ion density was evidenced with a shadowgraphy diagnostic [21] following a single electron bunch driving wakefields.

When a bunch train is formed by self-modulation, it was shown in theory and simulations [18, 19] that the motion of ions leads to the crossing of plasma electron trajectories [22] late along the bunch train and plasma. This results in a loss of coherence in the collective motion of plasma electrons and therefore to a decrease in wakefield amplitude that imprints itself on the bunch during the self-modulation process.

In this *Letter*, we observe for the first time an effect caused by motion of ions on a bunch driving wakefields. As expected, the effect depends inversely on the ion mass. Since wakefields are driven by multiple bunches, simulation results indicate that the ponderomotive force causes the motion of ions. In this case, the effect is also expected to depend on the amplitude of the wakefields, as also observed. When large enough, motion of ions suppresses wakefields late along the bunch. This absence of fields manifests itself as ‘tail’ (late increase in beam density) on time-resolved images of the bunch, as predicted by previous simulation results [18, 19].

Measurements are performed at AWAKE (Advanced WAKEfield Experiment) at CERN. A schematic layout of the experiment is shown in Fig. 1. AWAKE uses a bunch of 400 GeV protons from the Super Proton Synchrotron (SPS) to drive wakefields over 10 m of plasma. The bunch contains $N_{p^+} = (0.7\text{--}3) \times 10^{11}$ protons, is focused to a transverse rms size $\sigma_{x_0, y_0} \approx 160 \mu\text{m}$ near the plasma entrance, and has an rms duration of $\sigma_\xi \approx 170$ ps. The bunch is much longer than $\tau_{pe} = 2\pi/\omega_{pe} \cong (10\text{--}3)$ ps ($n_{pe} \cong (1 - 10) \times 10^{14} \text{cm}^{-3}$, typical of these experiments) and undergoes the self-modulation instability (SMI) over the first few meters of plasma [23, 24]. The SMI results in the formation of a periodic bunch train with a spacing of $\approx \tau_{pe}$. This train drives wakefields resonantly along the bunch and plasma,

producing large amplitude wakefields.

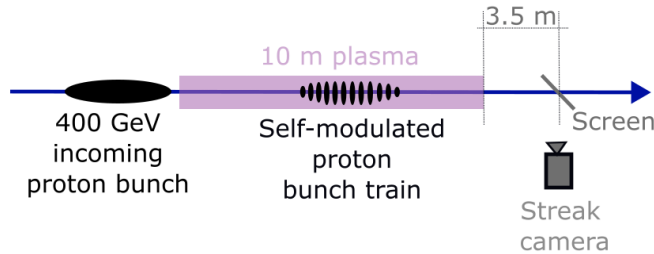


FIG. 1. Schematic of the experimental setup.

The plasma is provided by a pulsed DC discharge source [25, 26] and is either made of helium (^4He), argon (^{40}Ar) or xenon (^{131}Xe [27]) ($m_{\text{Ar}} \cong 10 \times m_{\text{He}}$ and $m_{\text{Xe}} \cong 3 \times m_{\text{Ar}}$). The discharge source has 0.2 mm aluminum windows at its entrance (and exit) that exclude the option of seeding with a relativistic ionization front [23, 28] or with a low-energy electron bunch [29]. Therefore, in these experiments, self-modulation grows from noise as an instability.

Gases are only partially and at most singly ionized [26]. The plasma density is adjusted by changing the gas pressure (8 to 45 Pa), the peak discharge current (300 to 600 A, pulse duration $\approx 25 \mu\text{s}$), or the timing between the discharge and the arrival time of the proton bunch, so that similar plasma densities can be reached with different gases. Reachable plasma density ranges are $n_{\text{pe}}=(0.1-4.8)\times 10^{14} \text{ cm}^{-3}$ with helium, $n_{\text{pe}}=(0.1-10)\times 10^{14} \text{ cm}^{-3}$ with argon, and $n_{\text{pe}}=(1-17)\times 10^{14} \text{ cm}^{-3}$ with xenon. Plasma densities are measured either by longitudinal, double-pass interferometry (prior to the experiment) or by the modulation frequency of the microbunch trains resulting from SMI [23, 30], and are averaged over the plasma length.

At a distance of 3.5 m downstream of the plasma exit, protons traverse a screen (150 μm thick SiO_2 , aluminum coated) and emit transition radiation (Fig. 1). Wavelengths in the $(450\pm 25) \text{ nm}$ range are imaged onto the entrance slit of a streak camera (with a width $\Delta y = 80 \mu\text{m}$), that provides time-resolved images of the bunch density distribution in a Δy -wide slice around its axis.

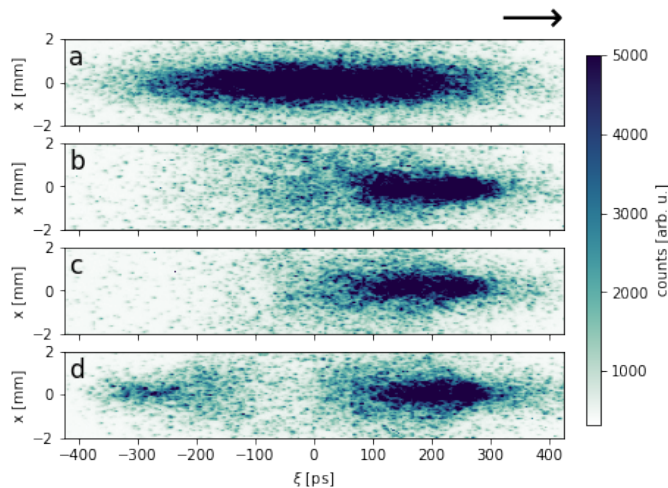


FIG. 2. Time-resolved proton bunch distribution $n_{p+}(x, \xi)$ with $N_{p+}=(2.8\pm 0.2)\times 10^{11}$ measured 3.5 m downstream of the plasma exit without plasma (a) and with 10 m of $n_{\text{pe}}=(4.8\pm 0.5)\times 10^{14} \text{ cm}^{-3}$ xenon (b), argon (c) and helium (d) plasmas (single measurement). The longitudinal bunch center is at $\xi = 0$. Bunches propagate to the right as indicated by the arrow on the top right. Color-scale saturated to highlight the bunch tail. Identical streak camera settings used for all measurements.

Figure 2a shows the measured proton bunch density $n_{p+}(x, \xi)$ with $N_{p+}=(2.8\pm 0.2)\times 10^{11}$ after propagation in vacuum (no plasma). The distribution is approximately bi-Gaussian with a transverse rms size of $\sigma_{x,y,\text{SC}} = 625 \mu\text{m}$ ($\gg \Delta y$). Figures 2b,c show the density after propagating in xenon (b) and argon (c) plasmas with $n_{\text{pe}}=(4.8\pm 0.5)\times 10^{14} \text{ cm}^{-3}$, the highest density reachable with helium. These show typical features of successful self-modulation [23, 24]: observable microbunch structure when using shorter time-windows (73 ps, not shown) [23]; decrease of the transverse bunch size (visible from the front of the bunch to $\xi \approx -250 \text{ ps}$), caused by adiabatic focusing

of the bunch in plasma [31]; signal decrease (visible for $\xi \lesssim 200$ ps, when compared to the no-plasma case on Fig. 2a), caused by the increase of proton divergence along the bunch [32]. The divergence increases because the transverse wakefield amplitude increases due to resonant wakefield excitation. Protons with larger transverse momentum diverge more during vacuum propagation downstream of the plasma exit, leading to a lower bunch density measured with the streak camera because of the effect of the slit. Very little to no signal is observed for $\xi \lesssim -100$ ps on Figs. 2b,c.

The bunch density measured with helium (Fig. 2d) closely resembles those with argon (Fig. 2c) or xenon (Fig. 2b) from the front of the bunch to $\xi \sim -100$ ps, showing essentially the same SMI development and wakefield growth along the bunch and plasma. Microbunches are visible with all three plasmas on shorter time-windows also in this case. However with helium (Fig. 2d) and for $\xi \lesssim -100$ ps, the bunch density increases again, leading to the appearance of a bunch tail, not present on Figs. 2b and c. This is the signature expected from the effect of the motion of ions on self-modulation [18, 19]. This occurs when the mass of the ions is sufficiently low and the amplitude of the wakefields is sufficiently high for motion of ions to suppress the wakefields in the back of the bunch. When wakefields are suppressed, protons acquire less transverse momentum, leading to much smaller divergence and increased proton bunch density, visible as a tail on the time-resolved image (Fig. 2d). The expected inverse dependence with m_i is confirmed, as only the bunch density measured with the lightest ions (helium) is disturbed. Simultaneous measurements with two streak cameras with orthogonal slits recording $n_{p^+}(x, \xi)$ and $n_{p^+}(y, \xi)$ (not shown) confirm that the core of the bunch and its tail are radially symmetric, as expected.

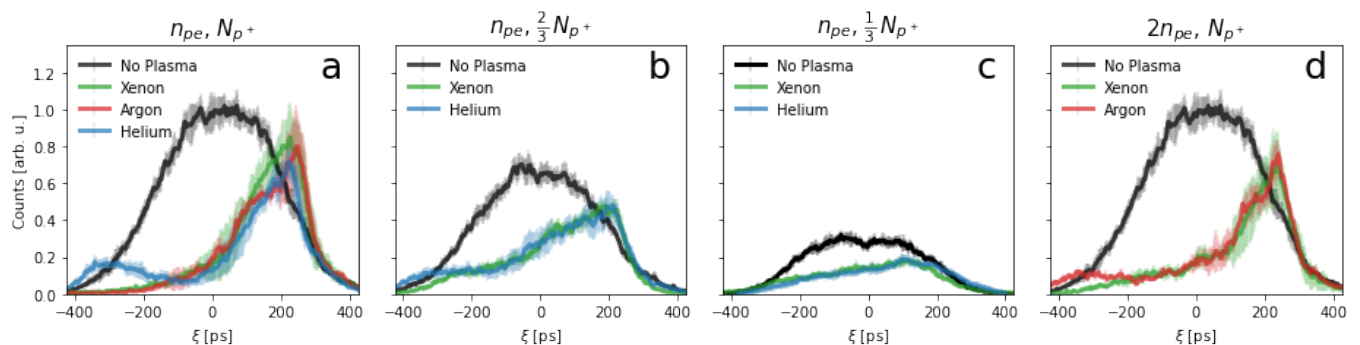


FIG. 3. Bunch density profiles $n_{p^+}(\xi)$ of time-resolved images using the range $|x| < 0.75$ mm of the $n_{p^+}(x, \xi)$ measurements. Each line represents the average of typically ten measurements. The standard deviation is shown by vertical error-bars. Bunches propagate to the right. Bunch and plasma parameters given in the titles and labels, with $n_{pe} = (4.8 \pm 0.5) \times 10^{14} \text{ cm}^{-3}$ and $N_{p^+} = (2.8 \pm 0.2) \times 10^{11}$.

The influence of motion of ions on self-modulation is also evident from bunch density profiles $n_{p^+}(\xi)$, presented in Fig. 3 as averages of typically ten measurements with their standard deviation. Figure 3a displays profiles corresponding to the four images on Fig. 2. These profiles again show the focusing effect in the front ($\xi \gtrsim 250$ ps), i.e., higher densities with plasma compared to without plasma (black line), as well as the presence of a clear tail in the distribution observed with helium (blue line $\xi \lesssim -100$ ps). The profiles highlight again the similarity of the bunch densities with all three plasmas between the front of the bunch and $\xi \sim -100$ ps. In that range, the development of self-modulation is primarily influenced by the response of the plasma electrons.

Figure 3b shows that with helium (blue line) and $\frac{2}{3}N_{p^+}$, i.e. a lower peak wakefield amplitude (decrease by approximately 1/3 in numerical simulation [33]; numerical simulations detailed later) and thus less motion of ions expected, the size of the tail is reduced when compared to that with N_{p^+} . Figure 3c shows that no tail is measurable with $\frac{1}{3}N_{p^+}$, i.e., with even lower wakefield amplitude (peak field in simulations approximately half of that with N_{p^+}). For Figs. 3b,c, we do not plot the lines obtained with argon, since there is no measurable difference with the ones with xenon (as is the case on Fig. 3a). These show that, for sufficiently low wakefield amplitude, achieved by decreasing N_{p^+} , the effect of motion of ions disappears even with the lightest ions.

Figure 3d shows that when increasing n_{pe} (by approximately a factor of two), the effect of motion of ions becomes observable with N_{p^+} and argon ($m_{\text{Ar}} \cong 10 \times m_{\text{He}}$). This is because of the higher amplitude of the wakefields (increase by $\sim 60\%$ in simulations compared to the ones with $n_{pe} = 4.8 \times 10^{14} \text{ cm}^{-3}$) and the shorter τ_{pe} (earlier decoherence for shorter τ_{pe}). We note that such a high density was not reachable with helium within the safe current limit of the pulse generator [25]. The effect observed with argon is similar to that observed at lower density using helium, showing that the same physics is at play. The fact that we still do not observe a tail with xenon (Fig. 3d, cyan line) shows that the amplitude of wakefields at this plasma density is now sufficient to make the bunch tail observable for argon (Fig. 3d, purple line), but not for xenon plasma ($m_{\text{Xe}} \cong 3 \times m_{\text{Ar}}$).

To confirm that the observed bunch tails result from the motion of ions [19], we conduct particle-in-cell simulations using 2D-cylindrical LCODE [34, 35] with input beam (bi-Gaussian proton bunch distribution) and plasma parameters from Fig. 2. The simulated proton bunch distributions are propagated in vacuum from the plasma exit to the location of the screen in the experiment (see Fig. 1). On Fig. 4, we display the density distributions of a Δy -wide slice (width of the camera slit) around the bunch axis for immobile ions (a) and mobile ions of xenon (b), argon (b) and helium (c).

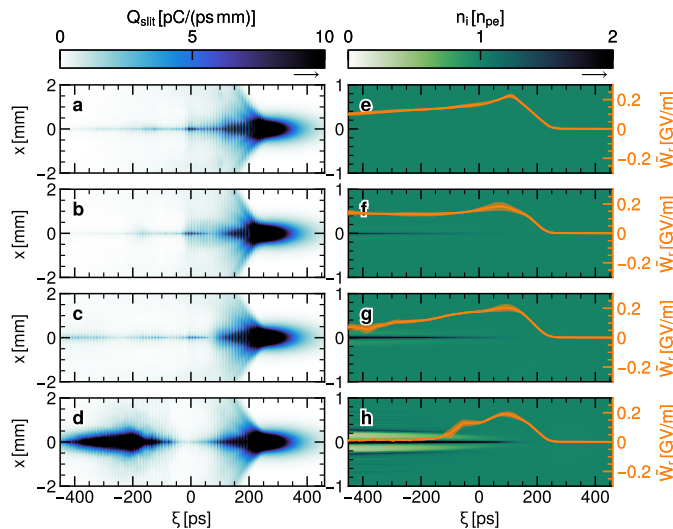


FIG. 4. Numerical simulation results (average of five simulations with different noise in the bunch particle distribution) with experimental parameters from Fig. 2. Figures a-d: bunch distributions at the location of the streak camera screen and with: immobile (a), xenon (b), argon (c), and helium (d) ions. Effect of the streak-camera slit included. Figures e-h: corresponding densities of plasma ions at the plasma exit ($z=10$ m). Orange lines: envelope of the transverse wakefields (W_r) at σ_{x_0, y_0} , also at $z=10$ m. Error-bars: standard deviation of the simulation results.

The SMI develops from noise in the randomly initiated drive bunch distribution, leading to variations in the results from simulation to simulation. For the density plots of Fig. 4 we show averages of five simulation results for different numerical seeds. For the amplitude of the transverse wakefields, we show the peak field values within one oscillation (envelope, orange lines) and standard deviations as error bars. As with experimental results (Fig. 2), we observe a clear bunch tail only with helium. Otherwise, distributions exhibit only subtle differences, which would be difficult to distinguish in experiments due to the finite temporal and spatial resolutions of the experimental images [32]. Simulated density profiles generally show higher density and longer bunch tails than experimental ones (Figs. 2d). This may imply that the initial wakefield amplitudes are larger in simulations than in experiments, as there are fewer particles in the simulations than in the experiment.

Nevertheless, profiles retain the same features and given the striking similarity between the bunch density distributions observed in simulations and experiments, we can deduce the underlying cause for the formation of the bunch tail from simulation results.

With mobile ions, ion density distributions (Figs. 4f-h) exhibit typical features caused by the ponderomotive force of wakefields driven by a narrow bunch [17, 18], rather than from the impulse response to the bunch. Since transverse wakefields are axially-symmetric and peak near σ_{x_0, y_0} from the axis, their ponderomotive force creates a high ion density region near the axis ($x \sim 0$ mm) and a low density surrounding it, especially visible with helium (Fig. 4h). This ion density perturbation changes the local plasma electron oscillation period, leading to a loss of coherence in their collective motion. The loss of coherence leads to a decrease of the wakefield amplitude in the back of the bunch ($\xi \lesssim -50$ ps on Fig. 4h), and therefore to the formation of a bunch 'tail' [17, 18].

The ion density perturbation is visible even with the heaviest ions (xenon, Fig. 4f), but becomes noticeable only very late along the bunch. Since in this case the relative density perturbation remains small, we observe no significant effect on the outcome of the self-modulation process. The effect occurs earlier and is larger with argon ions, but is too small for a tail to form.

In the absence of significant motion of ions (immobile ions and xenon Fig 4e,f) the wakefields maintain an approximately constant amplitude after saturation ($\xi \lesssim -100$ ps). With argon, the motion of ions is sufficient to cause a decrease in the wakefield amplitude for $\xi \lesssim -100$ ps, but not sufficient for a tail to form. With helium the wakefield amplitude plummets around $\xi \lesssim -50$ ps and thus a tail forms.

The slow decrease in wakefield amplitude observed with immobile ions later than $\xi \sim +100$ ps is due to the non-optimal evolution of self-modulation in a uniform plasma [10, 36]. This evolution also leads to the relatively small peak wakefield amplitudes (~ 200 MV/m) at 10 m, from ~ 600 MV/m at 6 m. Numerical simulation results suggest that with a plasma density step placed early along the plasma, wakefields maintain an amplitude close to their peak value [37, 38]. Interestingly, the small ion density perturbation observed with xenon (Fig. 4f) has a positive effect on the amplitude of the wakefields [20, 39, 40].

Usually in AWAKE, the plasma is made of Rubidium and simulation and experimental results indicate that the Rubidium ion mass ($m_{\text{Rb}} > 2 \times m_{\text{Ar}}$) is large enough for motion of ions not to have negative effects for any anticipated experimental parameters. Moreover, in acceleration experiments, the witness bunch would be placed at the earliest time along the bunch where wakefields reach their maximum amplitude (e.g., $\xi \simeq 0$ ps on Fig. 4f,g). Thus, motion of ions affecting wakefields later than that is irrelevant for the acceleration process. Tails such as those observed in these experiments were never observed with Rubidium, with densities up to $9.9 \times 10^{14} \text{ cm}^{-3}$.

We also note that the effect of the motion of plasma ions extends beyond that on bunch emittance and energy gain. It potentially imposes a limitation on the repetition rate of the acceleration process due to the time it takes for the energy of wakefields to dissipate [41] and correspondingly, the time the plasma takes to recover from the excitation-acceleration process that leaves energy in the plasma. This recovery time includes reaching again a uniform plasma density, i.e., uniform electron, ion, and neutral densities, as measured in Ref. [42].

The combination of experimental and simulation results presented in this *Letter* clearly show the effect of the motion of ions on the development of self-modulation, in line with expectations. This effect (formation of a bunch tail) is caused by the ponderomotive force of the wakefields. The experimental results confirm that the effect depends inversely on the mass of the ions (helium, argon, xenon), and depends directly on the amplitude of the wakefields (for a fixed ion mass). Simulation results show that the effect of motion of ions occurs later along the bunch than where wakefields reach their maximum amplitude. This is essential for future acceleration experiments at AWAKE aimed at reaching large electron bunch energy gain ($\cong 50$ GeV). The dependence observed with mass, and that with amplitude, are in agreement with those of theoretical and simulation models [18, 19]. These will be used to evaluate the possible effect of the motion of ions, e.g. in single and multiple drivers wakefield accelerators that may use light ions to avoid multiple ionization levels in the strong fields of the intense driver and witness beams.

I. ACKNOWLEDGEMENTS

This work was supported in parts by Fundação para a Ciência e Tecnologia - Portugal (Nos. CERN/FIS-TEC/0017/2019, CERN/FIS-TEC/0034/2021, UIBD/50021/2020), STFC (AWAKE-UK, Cockcroft Institute core, John Adams Institute core, and UCL consolidated grants), United Kingdom, the National Research Foundation of Korea (Nos. NRF-2016R1A5A1013277 and NRF-2020R1A2C1010835). M. W. acknowledges the support of DESY, Hamburg. Support of the Wigner Datacenter Cloud facility through the Awakelaser project is acknowledged. TRIUMF contribution is supported by NSERC of Canada. UW Madison acknowledges support by NSF award PHY-1903316. The AWAKE collaboration acknowledges the SPS team for their excellent proton delivery.

-
- [1] T. Tajima and J. M. Dawson, “Laser electron accelerator,” *Phys. Rev. Lett.*, vol. 43, pp. 267–270, Jul 1979.
 - [2] P. Chen, J. M. Dawson, R. W. Huff, and T. Katsouleas, “Acceleration of electrons by the interaction of a bunched electron beam with a plasma,” *Phys. Rev. Lett.*, vol. 54, pp. 693–696, Feb 1985.
 - [3] A. J. Gonsalves, K. Nakamura, J. Daniels, C. Benedetti, C. Pieronek, T. C. H. de Raadt, S. Steinke, J. H. Bin, S. S. Bulanov, J. van Tilborg, C. G. R. Geddes, C. B. Schroeder, C. Tóth, E. Esarey, K. Swanson, L. Fan-Chiang, G. Bagdasarov, N. Bobrova, V. Gasilov, G. Korn, P. Sasorov, and W. P. Leemans, “Petawatt laser guiding and electron beam acceleration to 8 GeV in a laser-heated capillary discharge waveguide,” *Phys. Rev. Lett.*, vol. 122, p. 084801, Feb 2019.
 - [4] I. Blumenfeld, C. E. Clayton, F.-J. Decker, M. J. Hogan, C. Huang, R. Ischebeck, R. Iverson, C. Joshi, T. Katsouleas, N. Kirby, W. Lu, K. A. Marsh, W. B. Mori, P. Muggli, E. Oz, R. H. Siemann, D. Walz, and M. Zhou, “Energy doubling of 42 gev electrons in a metre-scale plasma wakefield accelerator,” *Nature*, vol. 445, pp. 741–744, Feb 2007.
 - [5] $\tau_{pe} = 2\pi/\omega_{pe}$, with $\omega_{pe} = \sqrt{\frac{n_{pe}e^2}{\epsilon_0 m_e}}$, with c the speed of light in vacuum, n_{pe} the plasma electron density, e the electron charge, ϵ_0 the vacuum dielectric constant and m_e the electron mass.
 - [6] P. Muggli, V. Yakimenko, M. Babzien, E. Kallos, and K. P. Kusche, “Generation of trains of electron microbunches with adjustable subpicosecond spacing,” *Phys. Rev. Lett.*, vol. 101, p. 054801, Jul 2008.
 - [7] J. Cowley, C. Thornton, C. Arran, R. J. Shalloo, L. Corner, G. Cheung, C. D. Gregory, S. P. D. Mangles, N. H. Matlis, D. R. Symes, R. Walczak, and S. M. Hooker, “Excitation and control of plasma wakefields by multiple laser pulses,” *Phys. Rev. Lett.*, vol. 119, p. 044802, Jul 2017.

- [8] E. Esarey, J. Krall, and P. Sprangle, “Envelope analysis of intense laser pulse self-modulation in plasmas,” *Phys. Rev. Lett.*, vol. 72, pp. 2887–2890, May 1994.
- [9] P. Sprangle, J. Krall, and E. Esarey, “Hose-modulation instability of laser pulses in plasmas,” *Phys. Rev. Lett.*, vol. 73, pp. 3544–3547, Dec 1994.
- [10] N. Kumar, A. Pukhov, and K. Lotov, “Self-modulation instability of a long proton bunch in plasmas,” *Phys. Rev. Lett.*, vol. 104, p. 255003, Jun 2010.
- [11] A. Pukhov and J. Meyer-ter Vehn, “Laser wake field acceleration: the highly non-linear broken-wave regime,” *Applied Physics B*, vol. 74, pp. 355–361, Apr 2002.
- [12] J. B. Rosenzweig, A. M. Cook, A. Scott, M. C. Thompson, and R. B. Yoder, “Effects of ion motion in intense beam-driven plasma wakefield accelerators,” *Phys. Rev. Lett.*, vol. 95, p. 195002, Oct 2005.
- [13] D. H. Whittum, W. M. Sharp, S. S. Yu, M. Lampe, and G. Joyce, “Electron-hose instability in the ion-focused regime,” *Phys. Rev. Lett.*, vol. 67, pp. 991–994, Aug 1991.
- [14] T. Nechaeva, L. Verra, J. Pucek, L. Ranc, M. Bergamaschi, G. Zevi Della Porta, P. Muggli, R. Agnello, C. C. Ahcida, C. Amoedo, Y. Andrebe, O. Apsimon, R. Apsimon, J. M. Arnesano, V. Bencini, P. Blanchard, P. N. Burrows, B. Buttenschön, A. Caldwell, M. Chung, D. A. Cooke, C. Davut, G. Demeter, A. C. Dexter, S. Doebert, J. Farmer, A. Fasoli, R. Fonseca, I. Furno, E. Granados, M. Granetzny, T. Graubner, O. Grulke, E. Gschwendtner, E. Guran, J. Henderson, M. A. Kedves, S.-Y. Kim, F. Kraus, M. Krupa, T. Lefevre, L. Liang, S. Liu, N. Lopes, K. Lotov, M. Martinez Calderon, S. Mazzoni, K. Moon, P. I. Morales Guzmán, M. Moreira, N. Okhotnikov, C. Pakuza, F. Pannell, A. Pardons, K. Pepitone, E. Poimenidou, A. Pukhov, S. Rey, R. Rossel, H. Saberi, O. Schmitz, E. Senes, F. Silva, L. Silva, B. Spear, C. Stollberg, A. Sublet, C. Swain, A. Topaloudis, N. Torrado, M. Turner, F. Velotti, V. Verzilov, J. Vieira, C. Welsch, M. Wendt, M. Wing, J. Wolfenden, B. Woolley, G. Xia, V. Yarygova, and M. Zepp, “Hosing of a long relativistic particle bunch in plasma,” *Phys. Rev. Lett.*, vol. 132, p. 075001, Feb 2024.
- [15] V. E. Balakin, A. V. Novokhatsky, and V. P. Smirnov, “VLEPP: Transverse Beam Dynamics,” *Conf. Proc. C*, vol. 830811, pp. 119–120, 1983.
- [16] T. J. Mehrling, C. Benedetti, C. B. Schroeder, E. Esarey, and W. P. Leemans, “Suppression of beam hosing in plasma accelerators with ion motion,” *Phys. Rev. Lett.*, vol. 121, p. 264802, Dec 2018.
- [17] L. M. Gorbunov, P. Mora, and A. A. Solodov, “Dynamics of a plasma channel created by the wakefield of a short laser pulse,” *Physics of Plasmas*, vol. 10, pp. 1124–1134, 04 2003.
- [18] J. Vieira, R. A. Fonseca, W. B. Mori, and L. O. Silva, “Ion motion in self-modulated plasma wakefield accelerators,” *Phys. Rev. Lett.*, vol. 109, p. 145005, Oct 2012.
- [19] J. Vieira, R. A. Fonseca, W. B. Mori, and L. O. Silva, “Ion motion in the wake driven by long particle bunches in plasmas,” *Physics of Plasmas*, vol. 21, p. 056705, 05 2014.
- [20] R. I. Spitsyn, I. V. Timofeev, A. P. Sosedkin, and K. V. Lotov, “Characterization of wavebreaking time and dissipation of weakly nonlinear wakefields due to ion motion,” *Physics of Plasmas*, vol. 25, p. 103103, 10 2018.
- [21] M. F. Gilljohann, H. Ding, A. Döpp, J. Götzfried, S. Schindler, G. Schilling, S. Corde, A. Debus, T. Heinemann, B. Hidding, S. M. Hooker, A. Irman, O. Kononenko, T. Kurz, A. Martinez de la Ossa, U. Schramm, and S. Karsch, “Direct observation of plasma waves and dynamics induced by laser-accelerated electron beams,” *Phys. Rev. X*, vol. 9, p. 011046, Mar 2019.
- [22] J. M. Dawson, “Nonlinear electron oscillations in a cold plasma,” *Phys. Rev.*, vol. 113, pp. 383–387, Jan 1959.
- [23] E. Adli, A. Ahuja, O. Apsimon, R. Apsimon, A.-M. Bachmann, D. Barrientos, M. M. Barros, J. Batkiewicz, F. Batsch, J. Bauche, V. K. Berglyd Olsen, M. Bernardini, B. Biskup, A. Boccardi, T. Bogey, T. Bohl, C. Bracco, F. Braunmüller, S. Burger, G. Burt, S. Bustamante, B. Buttenschön, A. Caldwell, M. Cascella, J. Chappell, E. Chevallay, M. Chung, D. Cooke, H. Damerau, L. Deacon, L. H. Deubner, A. Dexter, S. Doebert, J. Farmer, V. N. Fedosseev, G. Fior, R. Fiorito, R. A. Fonseca, F. Friebel, L. Garolfi, S. Gessner, I. Gorgisyan, A. A. Gorn, E. Granados, O. Grulke, E. Gschwendtner, A. Guerrero, J. Hansen, A. Helm, J. R. Henderson, C. Hessler, W. Hofle, M. Hüther, M. Ibison, L. Jensen, S. Jolly, F. Keeble, S.-Y. Kim, F. Kraus, T. Lefevre, G. LeGodec, Y. Li, S. Liu, N. Lopes, K. V. Lotov, L. Maricalva Brun, M. Martyanov, S. Mazzoni, D. Medina Godoy, V. A. Minakov, J. Mitchell, J. C. Molendijk, R. Mompo, J. T. Moody, M. Moreira, P. Muggli, C. Mutin, E. Öz, E. Ozturk, C. Pasquino, A. Pardons, F. Peña Asmus, K. Pepitone, A. Perera, A. Petrenko, S. Pitman, G. Plyushchev, A. Pukhov, S. Rey, K. Rieger, H. Ruhl, J. S. Schmidt, I. A. Shalimova, E. Shaposhnikova, P. Sherwood, L. O. Silva, L. Soby, A. P. Sosedkin, R. Speroni, R. I. Spitsyn, P. V. Tuv, F. Velotti, L. Verra, V. A. Verzilov, J. Vieira, H. Vincke, C. P. Welsch, B. Williamson, M. Wing, B. Woolley, and G. Xia, “Experimental observation of proton bunch modulation in a plasma at varying plasma densities,” *Phys. Rev. Lett.*, vol. 122, p. 054802, Feb 2019.
- [24] M. Turner, E. Adli, A. Ahuja, O. Apsimon, R. Apsimon, A.-M. Bachmann, M. Barros Marin, D. Barrientos, F. Batsch, J. Batkiewicz, J. Bauche, V. K. Berglyd Olsen, M. Bernardini, B. Biskup, A. Boccardi, T. Bogey, T. Bohl, C. Bracco, F. Braunmüller, S. Burger, G. Burt, S. Bustamante, B. Buttenschön, A. Caldwell, M. Cascella, J. Chappell, E. Chevallay, M. Chung, D. Cooke, H. Damerau, L. Deacon, L. H. Deubner, A. Dexter, S. Doebert, J. Farmer, V. N. Fedosseev, G. Fior, R. Fiorito, R. A. Fonseca, F. Friebel, L. Garolfi, S. Gessner, I. Gorgisyan, A. A. Gorn, E. Granados, O. Grulke, E. Gschwendtner, A. Guerrero, J. Hansen, A. Helm, J. R. Henderson, C. Hessler, W. Hofle, M. Hüther, M. Ibison, L. Jensen, S. Jolly, F. Keeble, S.-Y. Kim, F. Kraus, T. Lefevre, G. LeGodec, Y. Li, S. Liu, N. Lopes, K. V. Lotov, L. Maricalva Brun, M. Martyanov, S. Mazzoni, D. Medina Godoy, V. A. Minakov, J. Mitchell, J. C. Molendijk, R. Mompo, J. T. Moody, M. Moreira, P. Muggli, E. Öz, E. Ozturk, C. Mutin, C. Pasquino, A. Pardons, F. Peña Asmus, K. Pepitone, A. Perera, A. Petrenko, S. Pitman, G. Plyushchev, A. Pukhov, S. Rey, K. Rieger, H. Ruhl, J. S. Schmidt, I. A. Shalimova, E. Shaposhnikova, P. Sherwood, L. O. Silva, L. Soby, A. P. Sosedkin, R. Speroni, R. I. Spitsyn, P. V. Tuv, F. Velotti, L. Verra, V. A. Verzilov, J. Vieira, H. Vincke, C. P. Welsch, B. Williamson, M. Wing, B. Woolley, and G. Xia, “Experimental observation of plasma wakefield growth driven by the seeded self-modulation of a proton bunch,” *Phys. Rev. Lett.*, vol. 122,

- p. 054801, Feb 2019.
- [25] N. E. Torrado, N. C. Lopes, J. F. A. Silva, C. Amoedo, and A. Sublet, “Double pulse generator for unipolar discharges in long plasma tubes for the awake experiment,” *IEEE Transactions on Plasma Science*, vol. 51, no. 12, pp. 3619–3627, 2023.
- [26] C. Amoedo and the AWAKE Collaboration, “Demonstration of proton bunch self-modulation in a discharge plasma source,” in preparation.
- [27] a mixture of: $^{129}\text{Xe} \sim 26.4\%$, $^{131}\text{Xe} \sim 21.2\%$, $^{132}\text{Xe} \sim 26.9\%$, $^{134}\text{Xe} \sim 10.4\%$.
- [28] F. Batsch, P. Muggli, R. Agnello, C. C. Ahdida, M. C. Amoedo Goncalves, Y. Andrebe, O. Apsimon, R. Apsimon, A.-M. Bachmann, M. A. Bastrukov, P. Blanchard, F. Braunmüller, P. N. Burrows, B. Buttenschön, A. Caldwell, J. Chappell, E. Chevally, M. Chung, D. A. Cooke, H. Damerau, C. Davut, G. Demeter, H. L. Deubner, S. Doebert, J. Farmer, A. Fasoli, V. N. Fedosseev, R. Fiorito, R. A. Fonseca, F. Friebel, I. Furno, L. Garolfi, S. Gessner, I. Gorgisyan, A. A. Gorn, E. Granados, M. Granetzny, T. Graubner, O. Grulke, E. Gschwendtner, V. Hafych, A. Helm, J. R. Henderson, M. Hüther, I. Y. Kargapolov, S.-Y. Kim, F. Kraus, M. Krupa, T. Lefevre, L. Liang, S. Liu, N. Lopes, K. V. Lotov, M. Martyanov, S. Mazzoni, D. Medina Godoy, V. A. Minakov, J. T. Moody, K. Moon, P. I. Morales Guzmán, M. Moreira, T. Nechaeva, E. Nowak, C. Pakuza, H. Panuganti, A. Pardons, A. Perera, J. Pucek, A. Pukhov, R. L. Ramjiawan, S. Rey, K. Rieger, O. Schmitz, E. Senes, L. O. Silva, R. Speroni, R. I. Spitsyn, C. Stollberg, A. Sublet, A. Topaloudis, N. Torrado, P. V. Tuev, M. Turner, F. Velotti, L. Verra, V. A. Verzilov, J. Vieira, H. Vincke, C. P. Welsch, M. Wendt, M. Wing, P. Wiwattananon, J. Wolfenden, B. Woolley, G. Xia, M. Zepp, and G. Zevi Della Porta, “Transition between instability and seeded self-modulation of a relativistic particle bunch in plasma,” *Phys. Rev. Lett.*, vol. 126, p. 164802, Apr 2021.
- [29] L. Verra, G. Zevi Della Porta, J. Pucek, T. Nechaeva, S. Wyler, M. Bergamaschi, E. Senes, E. Guran, J. T. Moody, M. A. Kedves, E. Gschwendtner, P. Muggli, R. Agnello, C. C. Ahdida, M. C. A. Goncalves, Y. Andrebe, O. Apsimon, R. Apsimon, J. M. Arnesano, A.-M. Bachmann, D. Barrientos, F. Batsch, V. Bencini, P. Blanchard, P. N. Burrows, B. Buttenschön, A. Caldwell, J. Chappell, E. Chevally, M. Chung, D. A. Cooke, C. Davut, G. Demeter, A. C. Dexter, S. Doebert, F. A. Elverson, J. Farmer, A. Fasoli, V. Fedosseev, R. Fonseca, I. Furno, A. Gorn, E. Granados, M. Granetzny, T. Graubner, O. Grulke, V. Hafych, J. Henderson, M. Hüther, V. Khudiakov, S.-Y. Kim, F. Kraus, M. Krupa, T. Lefevre, L. Liang, S. Liu, N. Lopes, K. Lotov, M. Martinez Calderon, S. Mazzoni, D. Medina Godoy, K. Moon, P. I. Morales Guzmán, M. Moreira, E. Nowak, C. Pakuza, H. Panuganti, A. Pardons, K. Pepitone, A. Perera, A. Pukhov, R. L. Ramjiawan, S. Rey, O. Schmitz, F. Silva, L. Silva, C. Stollberg, A. Sublet, C. Swain, A. Topaloudis, N. Torrado, P. Tuev, F. Velotti, V. Verzilov, J. Vieira, M. Weidl, C. Welsch, M. Wendt, M. Wing, J. Wolfenden, B. Woolley, G. Xia, V. Yarygova, and M. Zepp, “Controlled growth of the self-modulation of a relativistic proton bunch in plasma,” *Phys. Rev. Lett.*, vol. 129, p. 024802, Jul 2022.
- [30] M. Gross, J. Engel, J. Good, H. Huck, I. Isaev, G. Koss, M. Krasilnikov, O. Lishilin, G. Loisch, Y. Renier, T. Rublack, F. Stephan, R. Brinkmann, A. Martinez de la Ossa, J. Osterhoff, D. Malyutin, D. Richter, T. Mehrling, M. Khojayan, C. B. Schroeder, and F. Grüner, “Observation of the self-modulation instability via time-resolved measurements,” *Phys. Rev. Lett.*, vol. 120, p. 144802, Apr 2018.
- [31] L. Verra, E. Gschwendtner, and P. Muggli, “Adiabatic focusing of a long proton bunch in plasma,” 2022.
- [32] M. Turner and P. Muggli, “Understanding time-resolved images of awake proton bunches,” *Submitted to the Proceedings of EAAC 2023*, 2023.
- [33] Simulations use immobile ions and therefore represent peak wakefield amplitudes without motion of ions.
- [34] A. Sosedkin and K. Lotov, “Lcode: A parallel quasistatic code for computationally heavy problems of plasma wakefield acceleration,” *Nuclear Instruments and Methods in Physics Research Section A: Accelerators, Spectrometers, Detectors and Associated Equipment*, vol. 829, pp. 350–352, 2016. 2nd European Advanced Accelerator Concepts Workshop - EAAC 2015.
- [35] “Lcode.” <https://lcode.info>. Accessed: 2024-06-19.
- [36] C. B. Schroeder, C. Benedetti, E. Esarey, F. J. Grüner, and W. P. Leemans, “Growth and phase velocity of self-modulated beam-driven plasma waves,” *Phys. Rev. Lett.*, vol. 107, p. 145002, Sep 2011.
- [37] K. V. Lotov, “Physics of beam self-modulation in plasma wakefield accelerators,” *Physics of Plasmas*, vol. 22, p. 103110, 10 2015.
- [38] E. Gschwendtner, K. Lotov, P. Muggli, M. Wing, R. Agnello, C. C. Ahdida, M. C. Amoedo Goncalves, Y. Andrebe, O. Apsimon, R. Apsimon, J. M. Arnesano, A.-M. Bachmann, D. Barrientos, F. Batsch, V. Bencini, M. Bergamaschi, P. Blanchard, P. N. Burrows, B. Buttenschön, A. Caldwell, J. Chappell, E. Chevally, M. Chung, D. A. Cooke, H. Damerau, C. Davut, G. Demeter, A. C. Dexter, S. Doebert, F. A. Elverson, J. Farmer, A. Fasoli, V. Fedosseev, R. Fonseca, I. Furno, S. Gessner, A. Gorn, E. Granados, M. Granetzny, T. Graubner, O. Grulke, E. D. Guran, V. Hafych, A. Hartin, J. Henderson, M. Hüther, M. Kedves, F. Keeble, V. Khudiakov, S.-Y. Kim, F. Kraus, M. Krupa, T. Lefevre, L. Liang, S. Liu, N. Lopes, M. Martinez Calderon, S. Mazzoni, D. Medina Godoy, J. Moody, K. Moon, P. I. Morales Guzmán, M. Moreira, T. Nechaeva, E. Nowak, C. Pakuza, H. Panuganti, A. Pardons, K. Pepitone, A. Perera, J. Pucek, A. Pukhov, R. L. Ramjiawan, S. Rey, A. Scaachi, O. Schmitz, E. Senes, F. Silva, L. Silva, C. Stollberg, A. Sublet, C. Swain, A. Topaloudis, N. Torrado, P. Tuev, M. Turner, F. Velotti, L. Verra, V. Verzilov, J. Vieira, H. Vincke, M. Weidl, C. Welsch, M. Wendt, P. Wiwattananon, J. Wolfenden, B. Woolley, S. Wyler, G. Xia, V. Yarygova, M. Zepp, and G. Zevi Della Porta, “The awake run 2 programme and beyond,” *Symmetry*, vol. 14, no. 8, 2022.
- [39] V. A. Minakov, A. P. Sosedkin, and K. V. Lotov, “Accelerating field enhancement due to ion motion in plasma wakefield accelerators,” *Plasma Physics and Controlled Fusion*, vol. 61, p. 114003, oct 2019.
- [40] V. A. Minakov and K. V. Lotov, “Transformer ratio growth due to ion motion in plasma wakefield accelerators,” *Physics of Plasmas*, vol. 31, p. 034503, 03 2024.
- [41] R. Zgad Zaj, “Dissipation of electron-beam-driven plasma wakes,” *Nature Communications*, vol. 11, p. 4753, Sep 2020.

- [42] R. D’Arcy, J. Chappell, J. Beinortaite, S. Diederichs, G. Boyle, B. Foster, M. J. Garland, P. G. Caminal, C. A. Lindstrøm, G. Loisch, S. Schreiber, S. Schröder, R. J. Shalloo, M. Thévenet, S. Wesch, M. Wing, and J. Osterhoff, “Recovery time of a plasma-wakefield accelerator,” *Nature*, vol. 603, pp. 58–62, Mar 2022.